ELSEVIER

Journal of Chromatography A, 962 (2002) 29–40

JOURNAL OF CHROMATOGRAPHY A

www.elsevier.com/locate/chroma

Analysis of diffusion models for protein adsorption to porous anion-exchange adsorbent

Wei-Dong Chen, Xiao-Yan Dong, Yan Sun*

Department of Biochemical Engineering, School of Chemical Engineering and Technology, Tianjin University, Tianjin 300072, China

Received 29 January 2002; received in revised form 19 April 2002; accepted 23 April 2002

Abstract

The ion-exchange adsorption kinetics of bovine serum albumin (BSA) and γ-globulin to an anion exchanger, DEAE Spherodex M, has been studied by batch adsorption experiments. Various diffusion models, that is, pore diffusion, surface diffusion, homogeneous diffusion and parallel diffusion models, are analyzed for their suitabilities to depict the adsorption kinetics. Protein diffusivities are estimated by matching the models with the experimental data. The dependence of the diffusivities on initial protein concentration is observed and discussed. The adsorption isotherm of BSA is nearly rectangular, so there is little surface diffusion. As a result, the surface and homogenous diffusion models do not fit to the kinetic data of BSA adsorption. The adsorption isotherm of γ-globulin is less favorable, and the surface diffusion contributes greatly to the mass transport. Consequently, both the surface and homogenous diffusion models fit to the kinetic data of γ-globulin well. The adsorption kinetics of BSA and γ-globulin can be very well fitted by parallel diffusion model, because the model reflects correctly the intraparticle mass transfer mechanism. In addition, for both the favorably bound proteins, the pore diffusion model fits the adsorption kinetics reasonably well. The results here indicate that the pore diffusion model can be used as a good approximate to depict protein adsorption kinetics for protein adsorption systems from rectangular to linear isotherms.

Keywords: Diffusion models; Pore diffusion; Surface diffusion; Homogeneous diffusion; Parallel diffusion; Protein adsorption; Adsorption

1. Introduction

Ion-exchange and adsorption chromatography has been extensively employed for the recovery and purification of proteins [1,2]. To better understand the ion-exchange processes, it is necessary to investigate the process equilibrium, kinetics and hydrodynamics in detail [3,4]. It is well known that the diffusion of proteins into porous adsorbents and ion-exchange media is usually the rate-limiting step in the large-scale adsorption and ion-exchange processes [5,6], so research on protein intraparticle diffusion becomes to be an intriguing field in the fundamental studies of the separation processes.

Over the past decade or two, many articles have been published on this subject. In those studies, basically four types of models are frequently adopted, that is, pore diffusion model [7], surface diffusion model [8], homogeneous diffusion model [9,10] and parallel diffusion model [11,12]. Pore

*Corresponding author. Tel.: +86-22-2740-6590; fax: +86-22-2740-6590.

E-mail address: ysun@tju.edu.cn (Y. Sun).

0021-9673/02/$ – see front matter
PII: S0021-9673(02)00466-1

diffusion and homogeneous diffusion in liquid and gas phase adsorption systems and surface diffusion in gas phase adsorption systems have been well documented. However, limited research on the mechanisms of surface diffusion and parallel diffusion in liquid phase adsorption systems is reported. Liapis [13] assumed that in affinity chromatography, the surface diffusion was usually negligible, because there is strong interaction between the adsorbate and ligand and thus the pore diffusion was the rate-limiting step. With other adsorbents such as ion exchangers, the interaction may not be so strong as that for the affinity systems, so it is necessary to consider both the surface and pore diffusions at the same time, namely parallel diffusion [11] or two-phase diffusion [3]. Moreover, for a high-capacity adsorption system usually encountered in preparative separation processes, surface concentration and its gradient during the adsorption process may be higher than pore concentration and its gradient by orders of magnitude. Hence, even though the surface diffusivity is usually smaller than the pore diffusivity by one or two orders of magnitude [14], a high surface concentration gradient may result in a surface diffusion flux that is much greater than the pore diffusion flux. If a pore diffusion model is used to estimate pore diffusivity in such systems, the resulting value can be erroneously large, sometimes even larger than the diffusivity in infinitely diluted aqueous solution of protein (D_∞) [12,15]. Therefore, it is important that the parallel transport by pore and surface diffusions is considered for such systems.

Yoshida et al. [15] and Maekawa et al. [16] have studied the parallel transport of bovine serum albumin (BSA) by surface and pore diffusions based on the assumption that the bulk phase concentration of solute and the pore and surface diffusivities (D_p and D_s) are constant during the adsorption process. In the present work, we attempt to improve the parallel diffusion study on the basis of their results, along with analyzing the pore diffusion, surface diffusion and homogenous diffusion models. Dynamic batch adsorption of BSA and γ-globulin is carried out to investigate the validity and usefulness of these models, and the diffusivities of the proteins as a function of initial protein concentration are discussed.

2. Materials and methods

2.1. Materials

BSA (A-3912, minimum 96%) and γ-globulin (G-7516, purity approx. 99%) were purchased from Sigma (St. Louis, MO, USA). Anion exchanger, DEAE Spherodex M, was obtained from BioSepra (Cergy-Saint-Christophe, France). All other reagents are of analytical grade.

2.2. Adsorption equilibrium

Adsorption equilibrium experiments of BSA and γ-globulin on the anion exchanger were performed using the stirred batch adsorption method in 0.01 mol/l phosphate buffer (pH 7.6) at 25 °C. A known amount of the anion exchanger pre-equilibrated in the buffer was added to each of the flasks containing known volume of buffered protein solution with different concentrations (0.1–2.6 mg/ml). The flasks were shaken for 10 h in a shaking water bath at 25 °C, which is confirmed by the results of adsorption equilibrium studies to be sufficient to reach adsorption equilibrium under all the conditions studied [17]. The ion exchanger was then allowed to settle and the supernatant was filtered before determining the equilibrium protein concentration with a Model 9100 UV–Vis spectrophotometer at 280 nm. The amount of protein adsorbed to the DEAE Spherodex M was then calculated by mass balance.

2.3. Kinetics of batch adsorption

Adsorption kinetics of BSA and γ-globulin in the anion exchanger were performed in the phosphate buffer using the stirred batch adsorption method. Generally, 10 flasks each containing 20 ml of buffered protein solutions of the same concentration were pre-incubated in the shaking incubator at 25 °C, and exactly the same amount of the anion exchanger pre-equilibrated in the buffer was added to each flask. The mixture in the flasks was suspended in the incubator shaking at, unless stated otherwise, 170 rpm. The flasks were taken out successively from the incubator for supernatant measurement; about 5 ml

of the liquid in the flask was pumped out of the flask through a 2-μm stainless filter to determine the protein concentration. By this procedure, the time course of the liquid phase protein concentration decrease was determined. The protein concentrations were normalized by dividing the bulk phase concentration of protein (C), at time t, by the bulk phase concentration of protein at time zero (C_0).

2.4. Analysis and measurements

The particle size distribution of DEAE Spherodex M was measured with a Malvern Mastersizer 2000 particle analyzer (Malvern Instruments, Worcestershire, UK). The wet density of the medium was measured by a pycnometer at 25 °C. The effective intraparticle porosity of the DEAE Spherodex M for protein was determined using a batch diffusion technique [18]. The procedure is described as follows. Protein was buffered in 0.01 mol/l phosphate buffer, pH 7.6, with 0.5 mol/l sodium chloride. About 5–6 g of the anion exchanger (wet mass) pre-equilibrated in the buffer was added to flasks each containing 10 ml (V_L) of the buffered protein solution of a definite concentration. The flasks were incubated for 10 h in the shaking incubator at 170 rpm at 25 °C to allow partitioning equilibrium to be reached. It was confirmed by the results of adsorption equilibrium studies [17] that the proteins was not adsorbed to the anion exchanger under this condition. Then, the liquid phase protein concentrations were determined with the UV–Vis spectrophotometer at 280 nm, and the effective intraparticle porosity of the DEAE Spherodex M for protein is calculated by:

$$\epsilon_p = \frac{V_L}{V_S} \cdot \left(\frac{C_0 - C}{C} \right) \tag{1}$$

where V_S is volume of the wet gel used. Triplicate experiments were carried out at initial BSA concentrations of 0.5, 1.0 and 2.0 mg/ml and initial γ-globulin concentrations of 0.3, 0.8 and 1.3 mg/ml, respectively, and the effective intraparticle porosity values thus obtained were averaged and the standard deviations were determined.

3. Kinetic models

In this work, the adsorption kinetics of BSA and γ-globulin are analyzed by four diffusion models, that is, the pore diffusion, surface diffusion, homogeneous diffusion and parallel diffusion models. The models are constructed on the basis of the following assumptions [7,8,10,15].

(a) The adsorbent particles are spherical, with uniform size and density, and the functional groups of the ion exchanger are evenly distributed throughout the interior surface of the particle.

(b) The void fraction of the ion exchanger for a protein is constant during the adsorption process.

(c) Adsorption equilibrium can be represented by the Langmuir equation (Eq. (2)).

For the homogenous diffusion model, the protein concentration is in equilibrium with the concentration of the adsorbed protein on the external surface, while for the other three models, the protein concentration in the pores is in local equilibrium with the concentration of the protein adsorbed on the inner surface of the pore wall:

$$q = \frac{q_m C}{K_d + C} \tag{2}$$

3.1. Pore diffusion model

This model assumes that the driving force for intraparticle mass transfer is protein concentration gradient in the pore phase, and the protein adsorbed to the available binding sites in the pore walls remains fixed, that is, there is no surface diffusion. The governing continuity equation for the intraparticle mass transfer by pore diffusion is described as [7]:

$$\epsilon_p \frac{\partial C_p}{\partial t} + \frac{\partial q}{\partial t} = \frac{\epsilon_p D_{p,p}}{r^2} \cdot \frac{\partial}{\partial r} \cdot \left(r^2 \cdot \frac{\partial C_p}{\partial r} \right) \tag{3}$$

where $D_{p,p}$ is the pore diffusivity in the pore diffusion model.

In the batch adsorption system described above, the mass transfer of protein from the liquid phase to the solid phase is expressed by:

$$\frac{dC}{dt} = -\frac{3F\epsilon_p D_{p,p}}{R} \cdot \left(\frac{\partial C_p}{\partial r} \right)_{r=R} \tag{4}$$

The initial and boundary conditions for Eqs. (3) and (4) are as follows:

$$\text{IC:}\quad t=0,\ q=0,\ C_{\mathrm{p}}=0,\ C=C_0 \tag{5a}$$

$$\text{BC1:}\quad t=R,\ C_{\mathrm{p}}=C \tag{5b}$$

$$\text{BC2:}\quad r=0,\ \frac{\partial C_{\mathrm{p}}}{\partial r}=0 \tag{5c}$$

Eq. (5b) holds when the external liquid-film mass transfer resistance is negligible.

3.2. Surface diffusion model

Surface diffusion model assumes that surface diffusion is the rate-limiting step in the adsorption process. The governing continuity equation for the intraparticle mass transfer by surface diffusion is expressed as:

$$\epsilon_{\mathrm{p}}\frac{\partial C_{\mathrm{p}}}{\partial t}+\frac{\partial q}{\partial t}=\frac{D_{\mathrm{s,s}}}{r^2}\cdot\frac{\partial}{\partial r}\cdot\left(r^2\cdot\frac{\partial q}{\partial r}\right) \tag{6}$$

where $D_{\mathrm{s,s}}$ is the surface diffusivity in the surface diffusion model. Similar to the pore diffusion model, the mass transfer of protein from liquid phase to the solid phase is described by:

$$\frac{\mathrm{d}C}{\mathrm{d}t}=-\frac{3FD_{\mathrm{s,s}}}{R}\cdot\left(\frac{\partial q}{\partial r}\right)_{r=R} \tag{7}$$

The initial condition and the first boundary condition for Eqs. (6) and (7) are the same as Eqs. (5a) and (5b), while the second boundary condition is given by:

$$\text{BC2:}\quad r=0,\ \frac{\partial q}{\partial r}=0 \tag{8c}$$

3.3. Homogeneous diffusion model

In the homogeneous diffusion model, the adsorbent particle is considered as a homogeneous network, and the driving force for protein diffusion is the total protein concentration gradient in the adsorbent. Since the total concentration of protein in the adsorbent is:

$$Q=q+\epsilon_{\mathrm{p}}C_{\mathrm{p}} \tag{9}$$

the continuity equation for the intraparticle mass transfer by homogeneous diffusion is written as [10]:

$$\frac{\partial Q}{\partial t}=\frac{D_{\mathrm{e}}}{r^2}\cdot\frac{\partial}{\partial r}\cdot\left(r^2\cdot\frac{\partial Q}{\partial r}\right) \tag{10}$$

where D_{e} is the effective diffusivity. Similar to the above diffusion models, the mass transfer of protein from liquid phase to the solid phase is expressed by:

$$\frac{\mathrm{d}C}{\mathrm{d}t}=-\frac{3FD_{\mathrm{e}}}{R}\cdot\left(\frac{\partial Q}{\partial r}\right)_{r=R} \tag{11}$$

The initial and boundary conditions for this model is as follows:

$$\text{IC:}\quad t=0,\ Q=0,\ C=C_0 \tag{12a}$$

$$\text{BC1:}\quad r=R,\ Q=\frac{q_{\mathrm{m}}C}{K_{\mathrm{d}}+C} \tag{12b}$$

$$\text{BC2:}\quad r=0,\ \frac{\partial Q}{\partial r}=0 \tag{12c}$$

3.4. Parallel diffusion model

Parallel diffusion model assumes that pore and surface diffusions occur in parallel in an adsorbent particle. The intraparticle continuity equation for the model is described as [15]:

$$\epsilon_{\mathrm{p}}\frac{\partial C_{\mathrm{p}}}{\partial t}+\frac{\partial q}{\partial t}=\frac{\epsilon_{\mathrm{p}}D_{\mathrm{p}}}{r^2}\cdot\frac{\partial}{\partial r}\cdot\left(r^2\cdot\frac{\partial C_{\mathrm{p}}}{\partial r}\right)+\frac{D_{\mathrm{s}}}{r^2}\cdot\frac{\partial}{\partial r}\cdot\left(r^2\cdot\frac{\partial q}{\partial r}\right) \tag{13}$$

It is clear that the pore diffusion and surface diffusion models stated above are the two limiting cases of the parallel diffusion model, that is, Eq. (13) becomes the pore diffusion model (Eq. (3)) when $D_{\mathrm{s}}=0$ and the surface diffusion model (Eq. (6)) when $D_{\mathrm{p}}=0$.

In the case of parallel diffusion, the mass transfer of protein from the liquid phase to the solid phase can be written as:

$$\frac{\mathrm{d}C}{\mathrm{d}t}=-\frac{3F}{R}\cdot\left(\epsilon_{\mathrm{p}}D_{\mathrm{p}}\cdot\frac{\partial C_{\mathrm{p}}}{\partial r}+D_{\mathrm{s}}\cdot\frac{\partial q}{\partial r}\right)_{r=R} \tag{14}$$

The initial and boundary conditions described for the pore diffusion and surface diffusion models also hold for Eqs. (13) and (14).

3.5. Method of numerical solution

Along with their boundary conditions, the above model equations are solved by the orthogonal collocation method [19]. The number of collocation points in the radial direction of the adsorbent is set at 20; further increase in the number gave little influence on the simulation results.

4. Results and discussion

4.1. Results of preliminary experiments

The main factors influencing protein adsorption rate are the intraparticle diffusion and the external liquid-film mass transfer resistance [20,21]. In order for the study of the intraparticle diffusion, the effect of the liquid-film mass transfer on the adsorption rate has to be eliminated. Thus, dynamic adsorption of BSA was carried out at four shaking speeds from 100 to 170 rpm. The results showed that the liquid-film mass transfer resistance at 100 and 130 rpm could not be neglected. In contrast, the dynamic curves at 150 and 170 rpm almost overlapped, indicating that this mass transfer resistance for BSA is negligible under the conditions (data not shown). Because γ-globulin has smaller intraparticle diffusivities (see below), the liquid-film mass transfer resistance for γ-globulin can also be neglected at this shaking speed. Consequently, the dynamic adsorption experiments were carried out at 170 rpm in the following studies.

It was determined that the solid medium DEAE Spherodex M had a volume-weighted mean diameter of 83 μm and a wet density of 1.27 mg/ml. The effective intraparticle porosities of the medium for BSA and γ-globulin were measured to be 0.616 ± 0.023 and 0.440 ± 0.012, respectively. These data are used in the following model calculations.

Fig. 1 shows that the adsorption equilibrium data of BSA and γ-globulin to the anion exchanger can be well fitted to the Langmuir equation (Eq. (2)). Along with the physical properties of BSA and γ-globulin, the Langmuir equation coefficients (K_d and q_m) for BSA and γ-globulin obtained by nonlinear least-squares regression are summarized in Table 1.

It should be noted that γ-globulin used in this work was a polyclonal IgG, a mixture of different antibodies with p*I* values of 5.8 to 7.3, or an average p*I* value of 6.5 [25]. Thus, the isotherm parameters listed in Table 1 are the lumped values of the mixed antibodies. Moreover, the surface diffusivity of γ-globulin obtained below is considered as a lumped value because the binding strengths of the antibodies with different p*I* values might be different from each other. Due to the lack of large quantities of monoclonal antibodies for this kinetic study, γ-globulin was used as a high-molecular-mass model protein in comparison with BSA.

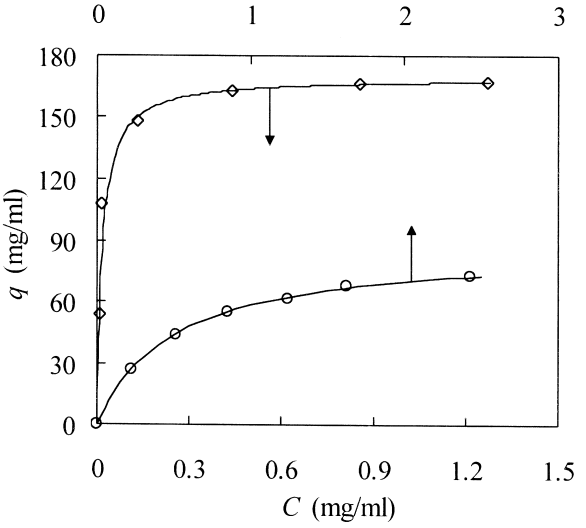

Fig. 1. Adsorption isotherms of (◇) BSA and (○) γ-globulin to DEAE Spherodex M. Solid lines are calculated from the Langmuir equation. The arrows indicate the abscissas for the corresponding data.

4.2. Determination of $D_{p,p}$, $D_{s,s}$ and D_e

The pore diffusion, surface diffusion and homogenous diffusion models are first analyzed because the diffusivities in these models can be separately determined by matching the theoretical curves with the experimental data using relevant models, as shown in Figs. 2 and 3. The diffusivities of BSA and γ-globulin thus obtained are summarized in Tables 2 and 3, respectively. Fig. 2 shows that the BSA concentration profiles can be well represented by the pore diffusion model, but the theoretical curves calculated from the surface diffusion and

Table 1
The physical properties and the Langmuir isotherm coefficients for the two proteins (25 °C)

Protein	M_r	pI	r_s (nm)	D_∞ (10^{-11} m^2/s)	q_m (mg/ml)	K_d (mg/ml)
BSA	67 000[a]	4.9[c]	3.59[a]	6.95[f]	169.5	0.017
γ-Globulin	158 000[b]	6.5[d]	5.59[e]	4.40[f]	87.7	0.50

[a] Data from Ref. [22].
[b] Data from Ref. [23].
[c] Data from Ref. [24].
[d] Data from Ref. [25], note that the value of 6.5 is an average pI value, since the γ-globulin used in this study is a polyclonal IgG, a mixture of different antibodies, and its pI values range from 5.8 to 7.3.
[e] Data from Refs. [22] and [23].
[f] Data from Ref. [26] and adjusted to 25 °C according to Stokes–Einstein equation.

homogeneous diffusion models deviate somewhat from the experimental data, especially under the conditions of lower initial BSA concentrations. The uptake profiles of γ-globulin predicted from the pore diffusion, surface diffusion and homogeneous diffusion models are displayed in Fig. 3. It is found that the three models can describe the dynamic process reasonably well. These results suggest that the pore diffusion may be dominant for BSA, while both the pore and surface diffusions work in parallel for γ-globulin. In addition, it can be seen from Tables 2 and 3 that $D_{p,p}$ decreases with increasing initial protein concentration, while $D_{s,s}$ and D_e ($\approx D_{s,s}$) show an opposite trend. These will be further discussed in the next section.

From Figs. 2 and 3, we find that the simulation curves from the surface diffusion model are completely overlapped with those from the homogeneous diffusion model, and values of $D_{s,s}$ are closely equal to values of D_e (Tables 2 and 3) for both the proteins. This result well reflects the intrinsic relationship between $D_{s,s}$ and D_e. As well documented in literature [10,27], use of q instead of Q in the

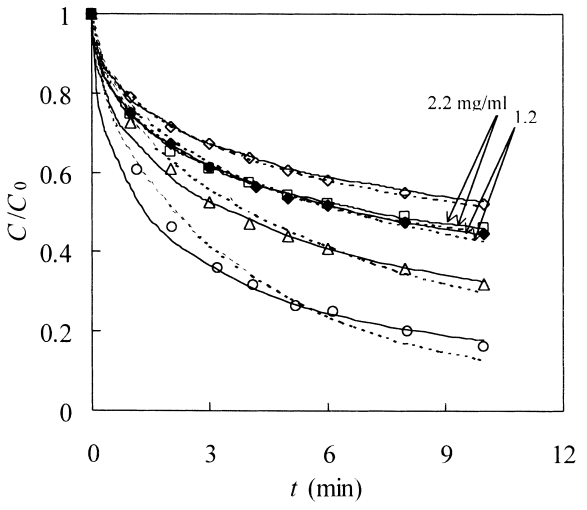

Fig. 2. Examples of experimental and simulated uptake curves of BSA. Solid lines are calculated from the pore diffusion model, and dotted lines are calculated from the surface diffusion model, which overlaps with those calculated from the homogeneous diffusion model. The initial concentrations of BSA are (○) 0.3, (△) 0.7, (♦) 1.2, (◇) 1.6, and (□) 2.2 mg/ml.

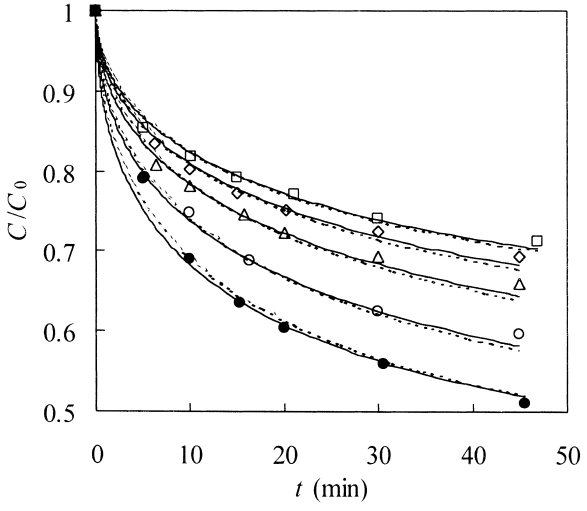

Fig. 3. Examples of experimental and simulated uptake curves of γ-globulin. Solid lines are calculated from the pore diffusion model, and dotted lines are calculated from the surface diffusion model, which overlaps with those calculated from the homogeneous diffusion model. The initial concentrations of γ-globulin are (●) 0.3, (○) 0.5, (△) 1.0, (◇) 1.3, and (□) 1.8 mg/ml.

Table 2
Experimental conditions and estimated model parameters for BSA

Run No.	C_0 (mg/ml)	α	β ($\cdot 10^{-4}$)	$D_{p,p}$ ($\cdot 10^{-11}$)	$D_{s,s}$ [a] ($\cdot 10^{-13}$)	$D_{s,1}$ [b] ($\cdot 10^{-17}$)	$D_{p,1}$ ($\cdot 10^{-11}$)	$D_{s,2}$ ($\cdot 10^{-15}$)	$D_{p,2}$ ($\cdot 10^{-11}$)	D_p ($\cdot 10^{-11}$)	D_p/D_∞
1	0.3	868.1	5.55	6.88	0.66					6.72	0.967
2	0.4	659.9	4.28	6.83	0.93					6.63	0.954
3	0.7	383.8	2.61	6.57	1.53					6.32	0.909
4	1.0	270.6	2.03	6.38	2.27	4.30	6.14	7.0	4.08	5.73	0.824
5	1.2	226.1	1.83	5.96	2.70					5.30	0.763
6	1.6	170.2	1.49	5.67	3.96					4.91	0.706
7	1.9	143.5	1.41	5.26	4.28					4.37	0.629
8	2.2	124.1	1.37	5.10	4.73					3.90	0.561

[a] $D_e \approx D_{s,s}$.
[b] $D_s = D_{s,1}$ in the calculation of D_p from the parallel diffusion model.

homogeneous diffusion model is insensitive to the change of simulation curves because q is much greater than $\epsilon_p C_p$, as is in this work (Fig. 1). As a result, the first term in the left-hand-side of Eq. (6) can be neglected, and Eq. (6) becomes identical to Eq. (10).

4.3. Determination of D_p and D_s in the parallel diffusion model

Assuming that the mass transfer rate from liquid phase to the solid phase calculated from the surface diffusion model (Eq. (7)) equals to that from the parallel diffusion model (Eq. (14)), we can obtain the following equation:

$$\left(D_{s,s} \cdot \frac{\partial q}{\partial r}\right)_{r=R} = \left(D_p \epsilon_p \cdot \frac{\partial C_p}{\partial r}\right)_{r=R} + \left(D_s \frac{\partial q}{\partial r}\right)_{r=R} \quad (15)$$

Rearranging the equation gives:

$$D_{s,s} = D_p \epsilon_p \cdot \frac{dC_p}{dq} + D_s \quad (16)$$

As an approximation, the relationship $dC_p/dq = C_0/q_0$ for a linear isotherm system can be derived [15]. Then, Eq. (16) is transformed into Eq. (17):

$$D_{s,s} = D_{p,1} \cdot \frac{1}{\alpha} + D_{s,1} \quad (17)$$

where

$$\alpha = \frac{q_0}{\epsilon_p C_0} \quad (18)$$

By plotting $D_{s,s}$ vs. $1/\alpha$, $D_{s,1}$ and $D_{p,1}$ can be determined from the intercepts and slopes of the straight lines, respectively (Fig. 4). The values of $D_{s,1}$ and $D_{p,1}$ thus obtained for BSA and

Table 3
Experimental conditions and estimated model parameters for γ-globulin

Run No.	C_0 (mg/ml)	α	β	$D_{p,p}$ ($\cdot 10^{-12}$)	$D_{s,s}$ [a] ($\cdot 10^{-14}$)	$D_{s,1}$ [b] ($\cdot 10^{-14}$)	$D_{p,1}$ ($\cdot 10^{-12}$)	$D_{s,2}$ ($\cdot 10^{-14}$)	$D_{p,2}$ ($\cdot 10^{-12}$)	D_p ($\cdot 10^{-12}$)	D_p/D_∞
1	0.3	249.2	0.83	7.60	3.40					4.87	0.111
2	0.4	221.5	0.82	7.21	3.52					4.39	0.100
3	0.5	199.4	0.81	6.79	3.60					3.97	0.090
4	1.0	132.9	0.62	5.90	4.91	1.62	4.23	1.70	3.15	3.50	0.080
5	1.3	110.8	0.56	5.09	5.40					3.22	0.073
6	1.6	94.9	0.48	4.92	6.06					3.21	0.073
7	1.8	86.7	0.44	4.65	6.50					3.20	0.073

[a] $D_e \approx D_{s,s}$.
[b] $D_s = D_{s,1}$ in the calculation of D_p from the parallel diffusion model.

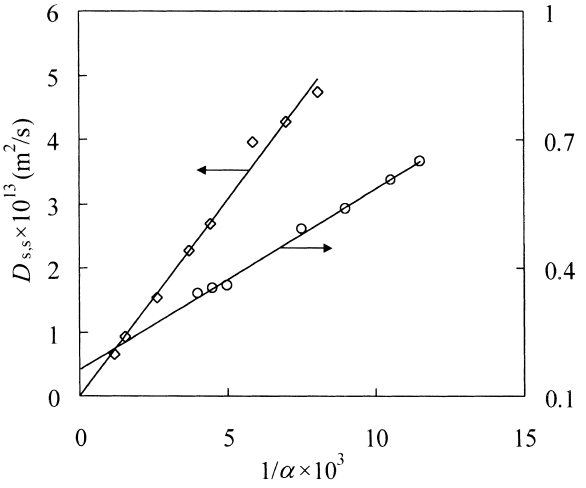

Fig. 4. The relationship between the surface diffusion coefficients ($D_{s,s}$), of (◇) BSA and (○) γ-globulin, and $1/\alpha$. The arrows indicate the ordinates for the corresponding data.

γ-globulin are also listed in Tables 2 and 3, respectively.

For the present nonlinear adsorption systems, surface and pore diffusivities may not be accurately predicted from the intercepts and slopes of the lines because of the use of the approximation $dC_p/dq = C_0/q_0$ [15]. Therefore, the intercepts and slopes are written as approximate surface and pore diffusivities, $D_{s,1}$ and $D_{p,1}$, respectively. We also found that the calculated dynamic adsorption curves from the parallel diffusion model using the values of $D_{s,1}$ and $D_{p,1}$ did not fit to the experimental data at initial concentrations of BSA$>$1.0 mg/ml and γ-globulin$>$0.5 mg/ml (data not shown).

The surface and pore diffusivities in the parallel diffusion model can be estimated from another approach. That is, by assuming that the mass transfer rate calculated from the pore diffusion model (Eq. (4)) is equal to that from the parallel diffusion model (Eq. (14)) [28], one has the following approximate relation:

$$D_{p,p} = D_{p,2} + \alpha D_{s,2} \quad (19)$$

As described by Maekawa et al. [28], the mass transport is controlled by the surface diffusion at large α values, while the mass transport is controlled by the pore diffusion at small α values. Thus, using Eq. (19) and the experimental data at small α values, the pore diffusivities for the parallel diffusion model can be determined from the intercepts of line 1 for both the proteins in Fig. 5. In addition, the slopes of line 2 for both the proteins in Fig. 5 in the range of larger α values give the values of surface diffusivities. Denoted as $D_{s,2}$ and $D_{p,2}$, their values for BSA and γ-globulin are indicated in Tables 2 and 3, respectively. Again, we found that the calculated dynamic curves from the parallel diffusion model using the values of $D_{s,2}$ and $D_{p,2}$ could not fit the experimental curves (data not shown).

For BSA in Table 2, $D_{s,2}$ is remarkably greater than $D_{s,1}$, and $D_{p,2}$ is about 30% smaller than $D_{p,1}$. These results may be caused by the fact that the pore diffusion is dominant for BSA, as stated earlier. For γ-globulin in Table 3, $D_{s,2}$ is approximately equal to $D_{s,1}$, and $D_{p,2}$ is about 25% smaller than $D_{p,1}$. Since both sets of the diffusion coefficients do not give accurate predictions of the dynamic adsorption curves for BSA and γ-globulin, it is considered that the traditional assumption that both the pore and surface diffusivities are constant for protein adsorption [11,15,28] may not be correct. However, we can assume that the surface diffusivity for a definite protein is constant according to the following

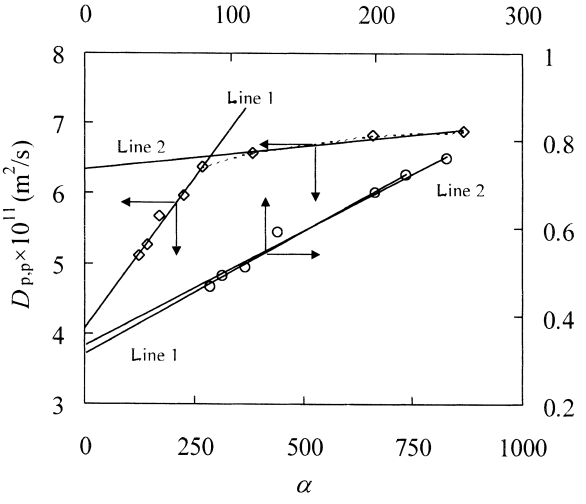

Fig. 5. The relationship between the pore diffusion coefficients ($D_{p,p}$), of (◇) BSA and (○) γ-globulin, and α. The arrows indicate the coordinates for the corresponding data.

reasons: (1) surface diffusivity in ion-exchange adsorption has been found to be a function of the concentration in the liquid at which the adsorption has one half of its maximum value [3], which corresponds to the K_d value in the Langmuir isotherm used in the present study. (2) In the case of γ-globulin that transports in parallel by surface and pore diffusions, the above-mentioned two approaches for the determination of the surface diffusivities resulted in nearly the same D_s value. (3) In the case of BSA that transport mainly by pore diffusion, the value of D_s is extremely small, so changing the value of D_s by keeping D_p unchanged do not produce satisfactory model prediction, as demonstrated by model simulation (data not shown). Usually, the D_s value determined by the first approach ($D_{s,1}$) is adopted as the surface diffusivity in the studies of parallel diffusion [11,15]. Hence, we also take $D_{s,1}$ as the surface diffusivities for BSA and γ-globulin. With the value of D_s, the pore diffusivity D_p is estimated by matching the parallel diffusion model with the dynamic adsorption data. As shown in Figs. 6 and 7, the experimental curves can be well depicted by the parallel diffusion model using a constant D_s and a changing D_p with initial protein concentration. The D_p values for BSA and γ-globulin are summarized in Tables 2 and 3, respectively.

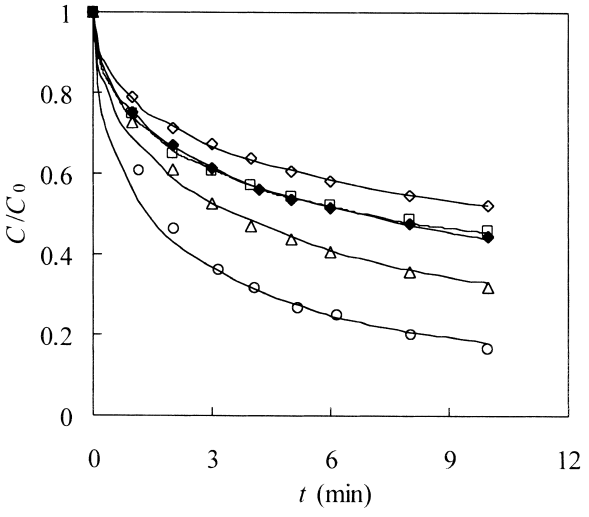

Fig. 6. Examples of experimental and simulated uptake curves of BSA. Solid lines are calculated from the parallel diffusion model using D_s and D_p listed in Table 2. The initial concentrations of BSA are (○) 0.3, (△) 0.7, (♦) 1.2, (◇) 1.6, and (□) 2.2 mg/ml.

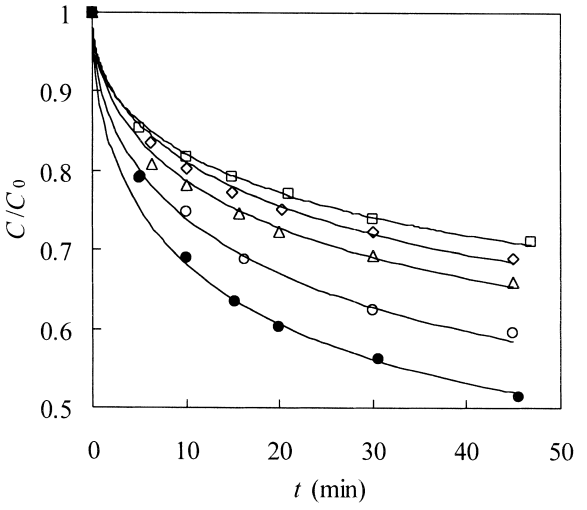

Fig. 7. Examples of experimental and simulated uptake curves of γ-globulin. Solid lines are calculated from the parallel diffusion model using D_s and D_p listed in Table 3. The initial concentrations of γ-globulin are (●) 0.3, (○) 0.5, (△) 1.0, (◇) 1.3, and (□) 1.8 mg/ml.

It is interesting to find that $D_{p,1}$ and $D_{p,2}$ stated above are the approximates of D_p at low and high initial concentrations, respectively. This is reasonable if one recalls the estimation approaches for $D_{p,1}$ and $D_{p,2}$. The first approach is accurate for the estimation of D_s at large α values (i.e., small C_0 values, see Eq. (18)) [28], so $D_{p,1}$ estimated by the first approach give more accurate fitting to the uptake profiles at low protein concentrations. In contrast, the value of $D_{p,2}$ is determined at small α values (i.e., large C_0 values), as shown by line 1 for both the proteins in Fig. 5, thus, $D_{p,2}$ is an approximate at high initial concentrations.

Furthermore, it can be seen from Tables 2 and 3 that the values of D_p/D_8 for BSA and γ-globulin are considerably different. This is definitely due to the remarkable difference between the physical properties of the two proteins (Table 1). The molecular mass and dimension of γ-globulin are much greater than those of BSA, so γ-globulin would encounter much larger hindrance effect than BSA.

As listed in Tables 2 and 3, the values of $D_{p,p}$ and

D_p for the two proteins decrease, while the values of $D_{s,s}$ (and D_e) for the two proteins increase, with increasing the initial protein concentration. Because the surface diffusion and homogenous diffusion models are far apart from the real mass transfer mechanisms of the two proteins, the apparent increase of $D_{s,s}$ and D_e in these models with increasing the initial protein concentration is simply attributed to the increased concentration gradient within the adsorbent with increasing the initial concentration. Thus, we concern more about the dependence of $D_{p,p}$ and D_p on the initial protein concentration. The decrease of $D_{p,p}$ with increasing the initial concentration has also been observed for the intraparticle diffusion of small molecules into activated carbon [29], but the reason was not discussed. For the present systems dealing with macromolecules, we consider that the decrease of the pore diffusivities with increasing the initial protein concentration is due to the increase of hindrance effect caused by the adsorption of protein. The pore size would become small upon protein adsorption, and higher initial protein concentration would result in higher protein adsorption density, leading to more significant decrease of the pore size near the adsorbent surface. When the adsorption became saturated at high initial concentrations, further increase of the initial concentration would not create additional decrease of the pore diffusivity. This can be observed from the D_p for γ-globulin (Table 3). Because the adsorption capacity of γ-globulin is much smaller than BSA (see Fig. 1 and Table 1), the adsorption of γ-globulin near the adsorbent surface would rapidly reach saturation in the adsorption process at $C_0 > 1.3$ mg/ml.

4.4. Suitability of the diffusion models for protein adsorption kinetics

The order of magnitude of D_s for BSA has been estimated at 10^{-17} m^2/s (Table 2), remarkably lower than that of D_p (10^{-11} m^2/s). It seems from the results that the adsorption kinetics of BSA in the ion exchanger is controlled by the pore diffusion. However, the degree of the contribution of the surface and pore diffusion to the intraparticle mass transport cannot be simply evaluated by the ratio of D_s to D_p [3,15]. Instead, it should be judged from the ratio of the mass transfer rate of surface diffusion to that of pore diffusion [15], that is:

$$\beta = \frac{\alpha D_s}{D_p} \tag{20}$$

Clearly, in the case of pore diffusion control, one has $\beta = 0$, and in the case of surface diffusion control, one has $\beta = \infty$. Yoshida et al. [15] indicated that when $\beta < 0.3$, the mass transport could be approximated by the pore diffusion model. As shown in Table 2, the values of β for BSA are lower than $6 \cdot 10^{-4}$. Thus, we can draw a conclusion that in the present adsorption system, the mass transport of BSA is controlled by pore diffusion. However, it should be noted that the pore diffusion model is still an approximate of the diffusion process, because, as can be seen from Table 2, the pore diffusivities estimated from the pore diffusion model is somewhat larger than those from the parallel diffusion model, particularly in the range of high initial concentrations. Hence, the pore diffusivity predicted from the pore diffusion model is still a lumped parameter that includes the contributions of both the pore and surface diffusions.

Yoshida et al. [15] reported the parallel diffusion of BSA in two chitosan-based anion exchangers, Chitopearl 2503 and 2507, assuming that D_p and D_s were constant during the adsorption process. The order of magnitude of D_p for BSA was 10^{-11} m^2/s, the same as in this work. However, the orders of magnitude of D_s for Chitopearl 2503 and 2507 were 10^{-13} and 10^{-14} m^2/s, respectively, much higher than those in the present work. Consequently, their values of β ranged from 1.72 to 9.54 for Chitopearl 2503, and from 0.115 to 0.875 for Chitopearl 2507, remarkably larger than those obtained in this work. This indicated the significant contribution of surface diffusion to the mass transport of BSA in the chitosan-based anion exchangers. These results may be caused by the fact that the values of K_d for BSA in their work (0.085 mg/ml for Chitopearl 2503, and 0.108 mg/ml for Chitopearl 2507) were five to six times larger than that in this work (0.017 mg/ml). It has been shown that surface diffusivity and the contribution of surface diffusion to mass transport increases with decreasing the binding strength of

protein [3,13], or with increasing the K_d value in the Langmuir isotherm.

On the basis of the above analysis of the effect of K_d on surface diffusion, it is understandable that the D_s value for γ-globulin is much larger than that for BSA, though the D_p value for γ-globulin is much smaller. As listed in Table 1, the value of K_d for γ-globulin is as large as 0.5 mg/ml, and β ranges from 0.44 to 0.83 in the concentration range studied. The results indicate that the surface diffusion of γ-globulin contributes greatly to the mass transport in the adsorption process, that is, the adsorption kinetics of γ-globulin is controlled by the parallel diffusion. In this case, both the pore diffusion and surface diffusion can reasonably depict the dynamic adsorption process, as shown in Fig. 3.

Xue and Sun [27] have reported that the adsorption kinetics of a linear adsorption system could be well fitted by both the pore diffusion and homogenous diffusion models. Combining their result with those obtained in this work, we can say that the pore diffusion model is a good approximate to describe the adsorption kinetics for the adsorption system with isotherms from rectangular to linear forms. In contrast, the surface diffusion model or the homogenous diffusion model is only valid for the system which adsorption isotherm is linear or less favorable. That is, the two models do not fit to the adsorption system of nearly rectangular isotherm.

5. Conclusions

In this article, four diffusion models have been analyzed for their suitability to depict the ion-exchange adsorption kinetics of proteins. We have shown here that the parallel diffusion model is a precise expression for the dynamic adsorption process, regardless of the form of the adsorption isotherms. However, the model is more complicated because there are two diffusivities that have to be determined. Because the pore diffusion model is a good approximate to describe the adsorption kinetics for the adsorption system with isotherms from rectangular to linear forms, the pore diffusion model can be employed as an alternative to replace the parallel diffusion model in practical applications such as process optimization and scale up.

6. Nomenclature

C	Protein concentration in bulk phase, mg/ml
C_0	Initial protein concentration in bulk phase, mg/ml
C_p	Protein concentration in pore, mg/ml
D_e	Effective diffusivity in homogeneous diffusion model, m^2/s
D_p	Pore diffusivity in parallel diffusion model, m^2/s
$D_{p,1}$	Pore diffusivity in parallel diffusion model obtained from the slope of the straight line shown in Fig. 4, m^2/s
$D_{p,2}$	Pore diffusivity in parallel diffusion model obtained from the intercept of line 1 shown in Fig. 5, m^2/s
$D_{p,p}$	Pore diffusivity in pore diffusion model, m^2/s
D_s	Surface diffusivity in parallel diffusion model, m^2/s
$D_{s,1}$	Surface diffusivity in parallel diffusion model obtained from the intercept of the straight line shown in Fig. 4, m^2/s
$D_{s,2}$	Surface diffusivity in parallel diffusion model obtained from the slope of line 2 shown in Fig. 5, m^2/s
$D_{s,s}$	Surface diffusivity in surface diffusion model, m^2/s
D_∞	Diffusivity of protein in infinitely dilute solution, m^2/s
F	Volumetric ratio of solid phase to liquid phase
K_d	Dissociation constant for Langmuir isotherm, mg/ml
M_r	Molecular mass
q	Adsorbed protein density, mg/ml
q_0	q in equilibrium with C_0, mg/ml
q_m	Adsorption capacity in Langmuir isotherm, mg/ml
Q	Adsorbed protein density in homogeneous network, mg/ml
r_s	Stokes radius, nm
R	Mean particle radius, m
t	Time, min
V_L	Volume of solution, ml
V_S	Volume of wet gel, ml
α	$q_0/\epsilon_p C_0$

β	$\alpha D_s/D_p$
ϵ_p	Effective intraparticle porosity for protein

Acknowledgements

This work is supported with the Natural Science Foundation of China (grant No. 20025617).

References

[1] E. Boschetti, J. Chromatogr. A 658 (1994) 207.
[2] J. Bonnerjea, S. Oh, M. Hoare, P. Dunnill, Bio/Technology 4 (1986) 954.
[3] J.A. Wesselingh, J.C. Bosma, AIChE J. 47 (2001) 1571.
[4] A.K. Hunter, G. Carta, J. Chromatogr. A 897 (2000) 81.
[5] G.L. Skidmore, B.J. Horstmann, H.A. Chase, J. Chromatogr. 498 (1990) 113.
[6] B.J. Horstmann, H.A. Chase, Chem. Eng. Res. Des. 67 (1989) 243.
[7] H. Pedersen, L. Furler, K. Venkatsubramanian, J. Prenosil, E. Stuker, Biotechnol. Bioeng. 27 (1985) 961.
[8] R.D. Tilton, C.R. Robertson, A.P. Gast, J. Colloid Interface Sci. 137 (1990) 192.
[9] L.E. Weaver, G. Carta, Biotechnol. Prog. 12 (1996) 342.
[10] P.R. Wright, F.J. Muzzio, B.J. Glasser, Biotechnol. Prog. 14 (1998) 913.
[11] M. Maekawa, K. Kasai, M. Nango, Colloids Surfaces A 132 (1998) 173.
[12] Z. Ma, R.D. Whitley, N.-H.L. Wang, AIChE J. 42 (1996) 1244.
[13] A.I. Liapis, Sep. Purif. Methods 19 (1990) 133.
[14] M. Suzuki, Adsorption Engineering, Elsevier, Amsterdam, 1990.
[15] H. Yoshida, M. Yoshikawa, T. Kataoka, AIChE J. 40 (1994) 2034.
[16] M. Maekawa, H. Nagai, K. Magara, Colloids Surfaces A 170 (2000) 191.
[17] W.-D. Chen, Y. Sun, J. Chem. Ind. Eng. (China) 53 (2002) 88.
[18] S. Zhang, Y. Sun, AIChE J. 48 (2002) 188.
[19] L.-Z. He, X.Y. Dong, Y. Sun, Biochem. Eng. J. 2 (1998) 53.
[20] D.C. Herak, E.W. Merrill, Biotechnol. Prog. 5 (1989) 9.
[21] A.I. Liapis, B. Anspach, M.E. Findley, Biotechnol. Bioeng. 34 (1989) 467.
[22] P.M. Boyer, J.T. Hsu, AIChE J. 38 (1992) 259.
[23] Q.C. Meng, Y.F. Chen, J. Chromatogr. 445 (1988) 29.
[24] E.M. Johnson, D.A. Berk, R.K. Jain, W.M. Deen, Biophys. J. 68 (1995) 1561.
[25] G. Garke, R. Hartmann, N. Papamichael, W.D. Deckwer, F.B. Anspach, Sep. Sci. Technol. 34 (1999) 2521.
[26] M.T. Tyn, T.W. Gusek, Biotechnol. Bioeng. 35 (1990) 327.
[27] B. Xue, Y. Sun, J. Chromatogr. A 921 (2001) 109.
[28] M. Maekawa, K. Murakami, H. Yoshida, J. Colloid Interface Sci. 155 (1993) 79.
[29] B.A. Duri, G. Mckay, J. Chem. Technol. Biotechnol. 55 (1992) 245.